21 Sept. 1976

HODOSCOPE IN-SITU RADIOGRAPHY*

by

E. Rhodes, A. De Volpi, C. Fink, G. Stanford, and R. Stewart

Reactor Analysis and Safety Division
Argonne National Laboratory
Argonne, Illinois 60439

ABSTRACT

The fast-neutron hodoscopes at TREAT and proposed for STF can be adapted to perform high-resolution radiography, in addition to their role of time-resolved test fuel imaging. Time resolution may be traded for increased spatial resolution by remote motorized scanning of the collimator, simultaneous collection of data from the detector array over extended time intervals, and deconvolution of the data from the collimator response function. Calculations and analysis of initial scanning experiments at TREAT indicate that an acceptable level of fuel density resolution can be achieved for TREAT and STF in-situ radiography.

I. INTRODUCTION

Following destructive transients at TREAT, test capsules are removed and typically radiographed by thermal neutron and x-ray transmission and by autoradiography. Radiographs are performed on the intact test capsule and at later stages of disassembly, in order to provide a preliminary view of the outcome of the experiment and to obtain images useful for post-test stripping, sectioning, and examination.[1] Radiography will also be necessary following STF transients.

The disposition of material in the test capsule can easily be disturbed after the transient and prior to radiography, due to mechanical stresses caused by handling, cooling, and sodium re-entry. Disagreement of final hodoscope fuel images with radiographs for some TREAT transients provides evidence that such disturbances occur. The lack of a correct detailed radiograph of the final disposition of material can confuse interpretation of the detailed metallurgical examination. The larger STF test capsules are likely to be even more susceptible to such disturbances.

There are two further limitations of present radiographic techniques which can lead to misinterpretation of results.[1] For larger test assemblies, low energy neutrons and photons penetrate the material only far enough to produce mainly surface features (ie. shadowgraphs), while true material volume density is needed. In addition, at best only density variations are recorded, no distinction being made between fuel, steel, and sodium. For many transients, the final disposition of material has mixed components and bears little resemblance to the initial configuration, and so the radiograph is subject to ambiguity. These limitations will be more severe for the STF test assemblies, which will be considerably larger than those used at TREAT.

---

*Work performed under the auspices of the U. S. Energy Research and Development Administration.

The question arises as to whether the facility imaging device for material motion detection during transients (the hodoscope, in the case of TREAT[2]) can provide in-situ radiographs immediately following transients, thereby minimizing disturbances to the test capsule prior to radiography. If this device detects fast neutrons emitted by the test fuel (such as the TREAT hodoscope), it is capable of providing needed volume density distinction of fuel, as well. Recent experiments[3] with the TREAT hodoscope indicate that a distinctive steel signature can be obtained by detection of high energy capture γ-rays emitted by the steel components, to the point of clad blockage monitoring. Thus, volume density distinction of steel is also possible. Ex-core radiography would continue to be performed where favorable, but would be supplemented (and in some cases, perhaps supplanted) by in-situ radiography.

II. HODOSCOPE IN-SITU RADIOGRAPHY REQUIREMENTS

The current 122 cm hodoscope at TREAT provides horizontal and vertical detection channel separations of 6.6 mm and 34.5 mm, respectively,[4] with a hodoscope spatial response function FWHM of $\sim$6 mm and $\sim$20 mm, respectively. The channels are arranged in an array of 10 columns of 36 rows. Table 1 shows the projected capability of an STF hodoscope for multi-subassembly tests,[5] indicating horizontal and vertical channel separation of 2 cm and 5 cm, respectively. Although the degree of spatial resolution necessary to provide useful in-situ radiographs is not firmly established, it would be expected to be considerably finer than provided by a hodoscope. Any fuel-motion detection device successfully meeting STF fuel-motion detection criteria would probably provide little more spatial resolution than the "necessary" level, due to the space-time resolution trade-off required to detect a minimum number of counts per pixel in a time-resolved interval. However, since no time resolution is required for radiography, time resolution may be traded for space resolution by scanning the hodoscope in small increments between channels horizontally and vertically, collecting enough counts at each point to provide a recognizable image. The increased spatial resolution is to be provided by deconvoluting the data from the hodoscope response function.

1. Hardware

The reactor power must be limited to its steady-state range ($\lesssim$ 80 KW for TREAT), and must be low enough that enough heat is not generated in the test capsule during the radiographic scan to change the disposition of the material. The capsule will have limited capability to dissipate heat, since coolant flow is not allowable. Count rates will be low and total scanning time will be relatively long and will need to be minimized. It may be necessary to separately monitor the capsule temperature (recognizing that the transient may have destroyed all interior thermocouples normally instrumented). In order to reduce the total scanning time to a reasonable value, data should be collected from all detection channels for each scan position. The neutron (fuel) and γ-ray (steel) data would be collected simultaneously at each scan point. Overlapping adjacent channels in the scan will allow determination and correction of individual channel responses. The basic existing (or planned) data acquisition system can be used, since it must be capable of collecting a large amount of data for the transient itself, but it must be modified to accept data in a different format and to cover a much longer time interval.

TABLE 1. HODOSCOPE FUEL MONITORING CAPABILITY FOR STF-MS TESTS

Requirement	Capability	Criterion Achieveable
Field of View		
Height	180 cm	Desirable
Width	30 cm	Desirable
Depth	30 cm	Desirable
Channel Intervals (Spatial Resolution)		
Height	5 cm	Desirable
Width	2 cm	Desirable
Depth	2 cm	Desirable
Mass Resolution	80 g	Better than Necessary Poorer than Desirable
Time Resolution		
30,000 MW	0.1 msec	Necessary
3,000 MW	1.0 msec	Necessary

The provision for scanning the hodoscope collimator (or the test capsule) horizontally and vertically in precise, reproducible increments must be designed into the system. The total scanning time required will be reduced substantially by the (necessary) integration of automatic (preferably computer-controlled) remote scanning into the data acquisition system. This would automatically increment the hodoscope collimator in a preprogrammed sequence, using stepping motors.

It would be desirable to integrate the readout of one of the reactor power monitors into the data acquisition system, to supplement the hodoscope side-channels used for transient power normalization.[4] It would be desirable as well to have an on-line computer with scope and hard copy graphics capability for limited real-time data analysis and facsimile transmission, in order to check operation during the scans and provide preliminary results.

2. Data Processing

The data is in digital form, which is an advantage over normal radiography, because the data is directly compatible with quantitative analysis and computer processing. (A normal radiograph must be scanned and converted to density values to be of quantitative use, a process hampered by film nonlinearity). Data analysis programs and techniques used for transient analysis can be applied to the scan data with minor modification.

The data must be corrected for reactor power normalization, test capsule power profile, spurious noise, and individual channel response differences, all of which are corrections applied to transient data as well.[4] The data is then in form for digital deconvolution, after which it can be displayed, in hodograph or profile form for example,[4] like transient data. Steel and fuel data can be superimposed. Pre-test as well as post-test scans can be performed, and difference data between the two can be displayed. (The pre-test scan could be used also to calibrate the detectors and center the collimator). Image enhancement techniques, such as background subtraction, differencing, and filtering, are easily applied, if desired. The data processing can be performed off-line or on-line, depending on available facilities. Real-time processing, though not essential, would be desirable.

III. DECONVOLUTION

The key to success of hodoscope in-situ radiography is the ability to deconvolute the scan data from the hodoscope spatial response function to produce an image of the desired spatial and density resolution. (By density resolution is meant the sensitivity to a count rate change caused by a given density change, at a given confidence level. Density resolution is higher if the number of counts collected per channel is higher.)

Deconvolution entails accurate determination of the hodoscope spatial response function, at least to much better accuracy than the desired image accuracy. To first order, it may be calculated from the geometric optics of the collimator and assumes the form of a truncated four-sided pyramid for the TREAT 122 cm collimator design (with edge truncations in the vertical direction due to occultation by the front collimator), varying slightly from center to edge channels. Scattering changes the shape, particularly

near the edges of the function (producing tails), but the effect is difficult to calculate, as it depends on the neutron energy dependence of the reactor signal and of the detector and on the collimator geometry. The response function can be determined experimentally by scanning the hodoscope over an approximation to a point neutron source, such as a piece of fuel, inserted in the center of the reactor core, while the reactor operates at steady-state conditions. The dimensions of the source should be smaller than the desired resolution width, leading to a very low count rate, so that the scan could consume a great deal of time. Fortunately, the measurement need only be performed once.

For digital computation, the deconvolution integral equation translates into a set of linear inhomogeneous algebraic equations for the image count rates at the resolved points corresponding to the scan positions. These equations are easily solved in terms of discrete Fourier transforms.[5,6] Unfortunately, the solutions are usually unstable with respect to noise, particularly noise of high spatial frequency, and the random fluctuations of count statistics contain high frequency components. The instability increases, the greater the degree of resolution (and number of resolved points). This requires the number of counts per pixel to be greater than indicated by count statistics for construction of an image of given variance. A technique due to Hunt[6,7] obtains reduced variance at the expense of a biased image. The method is equivalent to a particular filter which attenuates high spatial frequencies. The technique will be successful if a large variance reduction can be obtained while introducing only a small image bias. In addition, there are more general techniques which can be applied to the instability.[8,9]

IV. TOMOGRAPHIC RESOLUTION

Inspection of Table 1 reveals a depth resolution criterion of 2 cm for fuel motion in the STF-MS tests, equal to the horizontal resolution criterion. A similar depth resolution requirement exists for other STF tests. Presumably, depth resolution (but much finer) will be required for STF radiography also, to remove ambiguity in the final disposition of material in the large test assemblies.[5]

It is proposed to attain depth resolution in STF tests for fuel motion monitoring by using two hodoscopes at right angles.[5] Each right angle view contains m lateral pixels for each vertical resolution segment plane, the count rates from each lateral pixel being related to the sum of the emitted radiation, or projection, from the m lateral pixels behind it. Since there are $\sim m^2$ total pixels for each vertical plane, one has only 2m equations in $\sim m^2$ unknown pixel count rates. From Table 1, m=30/2=15, so there are 30 equations in ~225 unknowns, a rather indeterminate system. However, it is hoped that by following the motion from known initial to known final configuration, application of physical constraints, comparison with computer accident codes, and use of suitable tomographic reconstruction algorithms[9-12], a reasonably unambiguous three-dimensional fuel motion picture will arise.

In the case of hodoscope in-situ radiography, if say a resolution increase of a factor of 10 (0.2 cm) for the STF-MS case were needed, one would have 300 equations in ~22,500 unknown pixel count rates, a highly indeterminate system. The spatial resolution attainable by application of physical constraints and computer code accident sequences cannot be expected to

be sufficient to remove the resulting ambiguity. What is needed are projections at other orientations to add a sufficient number of independent equations. These are obtained by rotating the test capsule in small discrete steps, scanning the collimator at each angle. This is a variation of CAT (Computerized Axial Tomography) scanning, a procedure well-developed in theory and practice in the field of nuclear medicine.[9-12] There is no general agreement, however, as to the exact number of view angles necessary for proper reconstruction, either in theory or practice. Different results are obtained for different situations, depending particularly on the amount of symmetry present in the object.[12] The use of $\sim m$ distinct orientations seems to be a good rule of thumb. With two hodoscopes at right angles, only $\sim m/2$ discrete rotations of the test capsule would be required. For STF tests, both pre- and post-test tomographic scans may be necessary to provide the initial and final configurations mentioned above as needed to aid in removing the ambiguity in fuel motion, as well as to satisfy post-test examination requirements. A large amount of memory and much computation will be required for tomographic reconstruction of in-situ radiographs, probably requiring the facilities of a large fast computer.

Noise instabilities can occur in tomographic reconstruction algorithms, just as in deconvolution. The amount of noise amplification varies greatly in practice, depending on object characteristics and the algorithm used, and for many algorithms is not completely understood in theory. One of the simplest algorithms, 'Fourier reconstruction,' is amenable to a theoretical treatment of noise. This algorithm generally produces faithful and artifact-free images, but is also relatively sensitive to noise, having a count noise amplification factor of $m/4n$ where n is the number of distinct orientations.[11] The noise amplification will generally be less for most other reconstruction algorithms. Noise-attenuation techniques similar to that mentioned in Sec. III can be applied to 'Fourier reconstruction.'[6,8,11]

V. LIMITATIONS

There are several limitations to hodoscope in-situ radiography associated with the attainable spatial and density resolution. The first to be examined is the measurement-time limitation. The time allowable for measurement is limited by the reactor availability, and perhaps, the heat input to the test capsule during post-test scans. A measurement time of several days would strain the schedule at TREAT but not at STF, since STF tests would be spaced farther apart in time. In TREAT scanning experiments performed after the R8 transient, test capsule heating was not a problem, as the temperature saturated at a safe value. Extensive calculations performed prior to the R8 test indicated that the probability for relocation of material in the test section during 80 KW steady state operation of the reactor would be very remote. This does not necessarily apply to STF tests, for which a separate analysis would be required.

The availability of a limited measurement time implies a trade-off between density resolution and spatial resolution. The number of counts N_o per pixel (signal plus background) required for detection of a fractional signal change $\gamma=\Delta S/S$ for a signal-to-background ratio $\alpha=S/B$ is given by count statistics as

$$N_o = \beta^2 \gamma^{-1}(1+\alpha^{-1})[1+2\gamma^{-1}(1+\alpha^{-1})] \qquad (1)$$

for a hodoscope, where β is a confidence level factor (β=1 is a 68% confidence level, β=2 is 95% confidence level). As a rule of thumb, it seems reasonable to require that the mass resolution per pixel for the in-situ radiograph be as great as that required for the associated transient (ie., if the spatial resolution of the radiograph is to be 10 times that for the transient, $\sim 10^2$ times more total counts than required for the transient will be needed for the entire planar image, or $\sim 10^3$ times more counts for a tomographic image). In Table 1, 80 g is given as the mass resolution for a 2 cm x 2 cm x 5 cm resolved volume for fuel motion in STF-MS tests , so that the detectable fractional mass change $\mu=\Delta M/M=80/300=0.10$. This figure is based on detection of neutron emission by a 3 MeV threshold detector of 3×10^{-3} efficiency (attainable with stilbene). Calculations[5] indicate that in this case $\gamma \approx \mu=0.10$ and $\alpha \approx 2.9$, so that $N_o \approx 375$ (assuming β=1). It will be assumed that 80 KW is the allowable steady state level of the STF reactor, as well as for the TREAT reactor (although it may prove to be considerably higher). The 3×10^{-3} efficiency detector is calculated to produce only $\sim$1 cps at 80 KW[5] in each channel. However, it may be possible to develop a 0.10 efficiency detector (with minimal reduction in α) for STF, which is highly desirable in order to extend the fuel motion time resolution to lower power for MS tests (see Table 1). The 0.10 efficiency detector would produce $\sim$33 cps per channel at 80 KW.

In Table 2 are compiled the measurement times for STF-MS tomographic in-situ radiographs for the 1 cps and 33 cps detectors, for 5 times and 10 times the transient spatial resolution. N_o=375 counts were required per channel for each scan step. Channels were fully overlapped one channel horizontally and vertically in order to continuously monitor the differences between adjacent channels, so that $4N_o$=1500 counts were required per pixel. This also allows for residual instabilities in deconvolution and tomographic reconstruction.[6,11] As suggested in Sec. IV, the number of orientations of the test capsule was taken equal to the number of lateral projections at any one orientation (75 for a resolution factor of 5 and 150 for a resolution factor of 10). Two hodoscopes at right angles were assumed to be mounted, reducing the total rotation of the test capsule to 90° (rather than 180°). A positioning time of 10 sec was assumed for each scan and angle step. It is seen that a spatial resolution even 5 times that of the transient may require too long a measurement time for the 3×10^{-3} efficiency detector, providing added impetus for the development of a 0.10 efficiency detector.

At a TREAT power level of 80 KW, each channel produces $\sim$20 cps for a 7-pin test assembly, with a signal-to-background ratio about the same as above. Thus for detection of a γ=0.10 fractional signal change, the same number of counts N_o is required as above. This value of γ appears reasonable for TREAT in-situ radiographs. Measurement times for TREAT in-situ radiographs have been calculated under the assumptions made for STF above (except that TREAT possesses only one operable hodoscope) and are given in Table 3. It is seen that planar radiographs of both 5 times and 10 times the transient spatial resolution can be obtained in a reasonable period, but that a tomographic radiograph of 10 times the transient resolution would consume too much time. The TREAT hodoscope has no provision for easily scanning the collimator vertically over the test capsule, so that the test capsule would have to be incremented vertically (in 10 sec steps) to obtain the vertical resolution of Table 3. A redesigned test assembly and containment vessel or redesigned collimator may be necessary for vertical scanning.

TABLE 2. MEASUREMENT TIMES FOR STF-MS TOMOGRAPHIC IN-SITU RADIOGRAPHS AT 80 KW

Resolution Mult. Factor	Width & Depth Resolution	Height Res.	Orien-tations	Angle Step	Scan Steps per Orientation	Meas. Time (1 cps)	Meas. Time (33 cps)
5	4 mm	10 mm	38	2.4°	100	17 da	1.0 da
10	2 mm	5 mm	75	1.2°	400	134 da	7.4 da

TABLE 3. MEASUREMENT TIMES FOR TREAT IN-SITU RADIOGRAPHS AT 80 KW

Resolution Mult. Factor	Width (& Depth) Resolution	Height Res.	Scan Steps (per orientation)	Meas. Time (planar)	Orien-tations	Angle Step	Meas. Time (tomographic)
5	1.32 mm	6.90 mm	100	48 min	50	3.6°	1.7 da
10	0.66 mm	3.45 mm	400	3.2 hr	100	1.8°	13.3 da

The measurement times indicated in Table 2 and 3 are probably conservative figures (provided the uncertainties in the calculations for STF are not too great). However, as a precaution, the worst potential case needs consideration. Suppose that $4N_o$ counts per pixel were just sufficient to compensate for deconvolution instability.[6] Then if straight 'Fourier reconstruction' were used to produce three-dimensional radiographs[11] (see Sec. IV), even the 0.10 efficiency detectors would require 2.8 days to radiograph an STF-MS assembly at 5 times the transient resolution, and a tomographic TREAT radiograph at 5 times the transient resolution would require 4 days. All other cases in Tables 2 and 3 would become infeasible.

Even if unlimited measurement time were available, certain limitations in spatial and density resolution must be considered. In hodoscope in-situ radiography, spatial resolution is ultimately limited by radiation scattering from the test capsule, the reactor background, accuracy of the hodoscope response function, collimator and test capsule positioning accuracy, and truncation buildup in the numerical algorithms (due to finite computer word size). Density resolution is ultimately limited by accuracy of correction for response differences of individual channels and by effects related to the fact that fuel fast-neutron emission (rather than fuel mass) is measured, such as flux depression, self-shielding, and spatial variations in reactor power.

VI. ALTERNATIVE TECHNIQUES

One can envision lowering a scanning apparatus into the reactor following a shutdown after the transient, in order to perform CAT. One might detect emitted γ-rays or neutrons transmitted by a source. In either case, the residual reactor background is likely to swamp the signal, and in neither case would volume sensitivity or distinction of fuel, steel, or sodium be attained (particularly for large STF test assemblies).

Another possibility is to provide a full reactor slot (instead of the half-slot needed by a neutron emission hodoscope) and install an electron beam accelerator to perform high energy x-radiography, in the hope of attaining high-resolution in-situ radiographs without time-consuming scanning. However, the high energies required, and the large scattering produced, by large STF test assemblies may necessitate a hodoscope-like collimator aperture in order to obtain a large enough signal-to-background ratio. In addition, it would be difficult to justify the high additional cost necessary for high-energy x-radiography on the basis of in-situ radiography alone. If, on the other hand, the accelerator equipment were already in place as a major part of the fuel motion diagnostic system, one must consider that it would provide detection of only density variations (no distinction between fuel, steel, and sodium). A separate system for fuel imaging, such as a fast-neutron hodoscope, would probably be needed for both fuel motion diagnostics and in-situ radiography.

One might also consider replacing the hodoscope collimator by a different aperture, such as a pinhole or coded aperture, which provides greater transmission for a given resolution, in the hope of decreasing the measurement time. By using such an aperture of the same resolution as the hodoscope, the count rate would increase. By using such an aperture of high resolution, along with a high-resolution detection system, scanning could be eliminated.

Calculations indicate that the signal-to-backgound ratio deterioration of such apertures, except possibly for the pinhole, more than offsets signal gain by a considerable margin.[13] The use of high-resolution position-sensitive detectors would produce a further substantial degradation in signal-to-background ratio.

VII. APPLICATION TO TREAT HODOSCOPE

For TREAT, in-situ radiography must be fit into an existing hardware and data processing system, rather than being designed in, as is possible with STF. However, hardware and software modifications which have been implemented to date and which are being contemplated are straightforward.[1] The readout from one of the TREAT reactor fission chamber power monitors has been integrated into a spare hodoscope electronic channel by use of a voltage-to-frequency converter. This allows more accurate power normalization over the relatively long measurement time required for in-situ radiography.

1. Interim Hardware Modifications

At the present time, neither the 51 cm nor the 122 cm hodoscope allows easy vertical scanning over the test capsule, and no mechanism for vertically incrementing the test capsule while the reactor is under power exists. In the absense of vertical scanning capability, effort has concentrated on horizontal scanning for experimental determination of the potential and limitations of hodoscope in-situ radiography. In the hodoscope data acquisition system for TREAT transient tests, digital pulses from each hodoscope channel are fed to a binary-coded lamp array, which is photographed by a high-speed framing camera.[2] This system is difficult to modify for camera synchronization at the very low framing rates required for scanning and does not allow real-time data inspection and analysis. Therefore, a lamp-array decoder strip, which senses the lamp images from 2 detection channels at a time, has been hung from a notched slide over the lamp array. The decoder output is fed into the microprocessor which normally controls the source positioner used for calibrating the 122 cm collimator detectors. This microprocessor has the capability for recording the position of the neutron calibration source and the detector count rate on a teletype printer and paper tape, as it automatically steps the source over the detector array. A program is fed from the teletype paper tape reader into this microprocessor to allow recording of the decoder data.

In operation, the collimator is incremented (cranked) manually to a new horizontal position as indicated on a dial readout, which is typed manually on the teletype and recorded on paper tape. The counts are then accumulated from each hodoscope channel by the transient data acquisition system over the desired time interval and displayed on the lamp panel. The decoder is moved manually from notch to notch over the lamp images corresponding to the desired channels, and its readout is automatically recorded on the teletype printer and paper tape. Operation is tedious and time-consuming (approximately a second per channel per scan position) but adequate for the purpose, provided not many of the 334 channels (including neutron and γ-ray channels) need to be decoded. In order to minimize the number of channels required, the policy up to the present time has been to scan a single column (36 neutron and 36 γ-ray channels) over the entire test capsule.

2. Present Data Processing

The scan data on the paper tape produced at TREAT is processed and analyzed at the ANL-East RAS minicomputer display and analysis station.[4] Programs normally used to process transient data have been modified for in-situ radiography. Program TPLT[4] was modified to produce single and composite graphs of the individual channel scans and vertical profiles on the electrostatic printer/plotter, including capabilities for power normalization and post-pre-transient scan difference plots. Program HGRF[4] was modified to produce intensity-modulated images of the required fine horizontal resolution on the display scope and the electrostatic printer/plotter. Program EFFI[4] was modified to provide channel efficiency and reactor power profile corrections for the scan data based on a least-squares fit to an expected count rate profile for a pre-transient scan.

In practice, pre- and post-transient scans are performed at TREAT. Using HGRF, TPLT, and TREAT printer output, the paper tape data are corrected for spurious effects. EFFI corrections determined from the corrected pre-transient data are then made and new HGRF and TPLT output are produced. Deconvolution of the adjusted data from the assumed hodoscope response function is the next step (the final step, if tomographic radiographs are not desired). A deconvolution program based on a modification of Hunt's method[6,7] is being written, but has not been completed.

Pre-transient neutron (test fuel) scan data for transient R9 and pre- and post-transient neutron (fuel) and γ-ray (steel) scan data for transient R8 have been obtained, at 1.2 mm intervals in the horizontal direction. Only the neutron data has been fully analyzed and is reported here. Correction for spurious effects, which were few in number, was easily done. Reactor power varied so little over the time span of measurement that power normalization, though provided, was hardly necessary. As found during transient tests, relative channel efficiencies were found to vary by factors of 3 (or less) at a reactor power level of 80 KW, despite pre-transient calibration.[4] However, even larger efficiency variations are routinely handled by EFFI successfully in transient analysis, although a reduction in this variation would undoubtedly lead to higher density resolution.

Two unexpected effects were encountered in the R8 and R9 scan data. First, it was found that relative signal-to-background ratios varied among individual channels. This effect was successfully corrected for by adding a second fitting parameter for each channel in EFFI, except that channels at the extreme top and bottom of the scanning column, which view no test fuel in the pre-transient scan, cannot be corrected. The density changes ascribed to any fuel relocated to the viewing area covered by these channels are somewhat uncertain. Second, the responses of several channels near the bottom of the scanning column were found to be too large (by a factor of 4 or less) in the R8 pre-transient scan. This was determined from a comparison of the (power normalized) background data for the pre- and post-transient scans (which should be the same). The responses of the remaining channels were judged to be unchanged. The count rates of the afflicted channels were adjusted in the R8 pre-transient scan to provide a (power-normalized) background equal to that of the post-transient scan.

Despite the difficulties with individual channel responses, satisfactory renditions of the scan data have been obtained which are suitable for deconvolution to the stipulated density resolution of 0.10 (see Sec. V). Graphs and a discussion of the R8 scan data may be found in the Appendix.

3. Future Plans

The anomalies in individual channel response for R8 and R9 neutron scans mentioned above are to be investigated, in order to reduce the effects and obtain greater potential density resolution. In addition, analysis and correction of the R8 γ-ray scans is to be completed, in preparation for deconvolution. Future TREAT transients will also be scanned.

The deconvolution program is to be completed and applied to the experimental scan data. In addition, computer experiments are planned in which simulated signal and background combinations will be convoluted with assumed hodoscope response functions, count fluctuations will be added using pseudo-random number routines, and the results will be deconvoluted and compared to the simulated test assemblies. These computer experiments are to be used to optimize the deconvolution process and determine its limitations. One effect to be examined is the sensitivity to inaccuracies in the hodoscope spatial response function. The response function will need to be determined to the required accuracy, which can probably best be done by a combination of scattering calculations and experimental verification and correction. Further comments on deconvolution are contained in the Addendum.

A new minicomputer-controlled magnetic disk data acquisition system, with magnetic tape data transfer unit, is to be installed on the TREAT hodoscope in the near future, replacing the present system, which will serve as a backup during transients. The new system will have 0.6 msec time resolution, will store over 3000 cycles of data, and will record the data on magnetic tape in digital form, eliminating the present necessity of development and scanning of photographic film.[2,4] This system can be used for controlling and recording the scan data for in-situ hodoscope radiography, but an additional disk or tape unit may be required. To complete the radiographic system, a remote motorized scanning apparatus controlled by the minicomputer is needed, along with a means for vertical scanning, either by incrementing the test capsule or the hodoscope collimator. If it is decided that tomographic radiographs are desired, a device for automatically incrementing the test capsule through a 180° rotation in small steps will also be necessary. Further desirable additions include hardware and software mentioned in Sec. II for real-time (or off-line) image construction, enhancement, and display.

REFERENCES

1. A. De Volpi, "High-resolution Fast-neutron and Gamma Digital Radiography," Proceedings of 1975 Nuclear Science Symposium, San Francisco, Cal. (19-21 November 1975).

2. A. De Volpi, R. J. Pecina, R. T. Daly, D. J. Travis, R. R. Stewart, and E. A. Rhodes, "Fast-Neutron Hodoscope at TREAT:Development and Operation," Nuclear Technology 27, pp 449-487 (November 1975).

3. A. De Volpi, C. L. Fink, and R. R. Stewart, "Monitoring Clad Blockages," Information Exchange Conference on Reactor Fuel- and Clad-Motion Diagnostics, Albuquerque, N. M. (November 1975).

4. A. De Volpi, R. R. Stewart, J. P. Regis, G. S. Stanford, and E. A. Rhodes, "Fast-Neutron Hodoscope at TREAT:Data Processing, Analysis, and Results," Nuclear Technology 30, pp. 398-421 (September 1976).

5. Experiment Needs and Facilities Study, Sec. 6:Experiment Diagnostics, ANL (drafted 22 June 1976).

6. B. R. Hunt, An Improved Technique for Using the Fast Fourier Transform to Solve Convolution-Type Integral Equations, LA-4515-MS (October 1970).

7. B. R. Hunt, Statistical Aspects of Deconvolution, LA-4556-MS (December 1970).

8. Arthur E. Hoerl and Robert W. Kennard, "Ridge Regression:Applications to Nonorthogonal Problems," Technometrics 12, pp 69-82 (February 1970).

9. Image Processing for 2-D and 3-D Reconstruction from Projections:Theory and Practice in Medicine and the Physical Sciences, Optical Society of America Technical Digest (4-7 August 1975, Stanford, California).

10. John W. Beattie, "Tomographic Reconstruction from Fan Beam Geometry Using Radon's Integration Method," IEEE Transactions on Nuclear Science 22 (February 1975).

11. L. A. Shepp and B. F. Logan, "The Fourier Reconstruction of a Head Section," IEEE Transactions on Nuclear Science 21 (June 1974).

12. T. F. Budinger and G. T. Gulberg, "Three-Dimensional Reconstruction in Nuclear Medicine Emission Imaging," IEEE Transactions on Nuclear Science 21 (June 1974).

13. E. Rhodes, private communication.

BLANK PAGE

APPENDIX

HODOSCOPE IN-SITU RADIOGRAPHY

In this appendix, the figures presented at the meeting are shown, along with a discussion. In Figure 1 is seen the layout of the TREAT reactor, showing the 51cm hodoscope collimator and neutron radiography facilities. In Figure 2 is shown a post-test neutron radiograph of TREAT Test E8, with a comparison to the dissection examination. The lack of volume distinction and material differentiation is obvious, even for a 7-pin test assembly. For large STF assemblies, it would be considerably worse.

A comparison of uncorrected pre-test horizontal scans in Figures 3 and 4 shows that both the efficiencies and signal-to-background ratios varied among individual detection channels in the R8 scans. Figure 5, the uncorrected post-test vertical background profile, displays the usual "truncated cosine" reactor power profile, while Fig. 6, the uncorrected pre-test vertical background profile, displays the anomalously high count rates observed in rows 29-35. A comparison of Figs. 7 and 8, the uncorrected and corrected pre-test vertical test fuel profiles, and of Figs. 6 and 9, the uncorrected and corrected pre-test vertical background profiles, indicates the corrections are adequate for reactor power profile, individual detector efficiencies and signal-to-background ratios, and anomalous pre-test count rates.

Figure 10, the corrected post-test overall vertical profile, when compared to Fig. 8, illustrates the fuel slumping from rows 5-18 into rows 29 and 30 which occurred during TREAT transient R8. The fuel relocation is exemplified in more detail in several graphs in which the post-test scan is subtracted from the pre-test scan. The fuel void in the upper part of the test assembly is seen in Fig. 11. Fig. 12 indicates more dispersal to the sides than slumping in the middle region of the test assembly, and Fig. 13 shows the accumulated fuel in the lower part of the test assembly. Two-dimensional fuel distribution information is presented in Figs. 14 and 15, which are corrected pre- and post-test intensity-modulated pseudo-radiographs. It should be noted that these results refer only to the static final distribution of fuel in the transient, with no reference to the sequence of fuel motion events leading to this distribution (which awaits analysis of hodoscope dynamic measurement data).

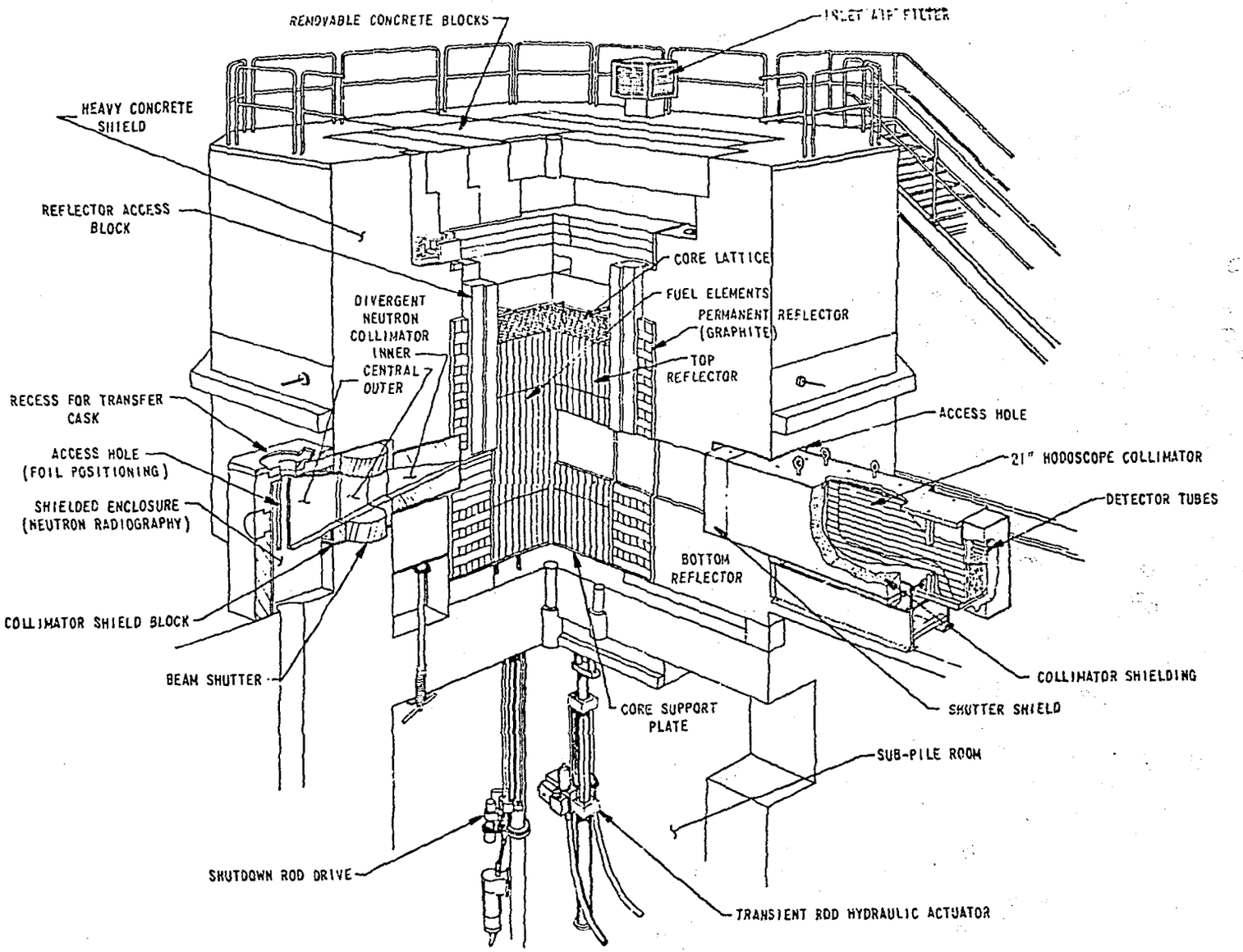

Fig. 1. Layout of TREAT reactor, showing 21" (51 cm) hodoscope at south face and neutron radiography facilities. A cross-focused 122 cm hodoscope is presently installed at north face.

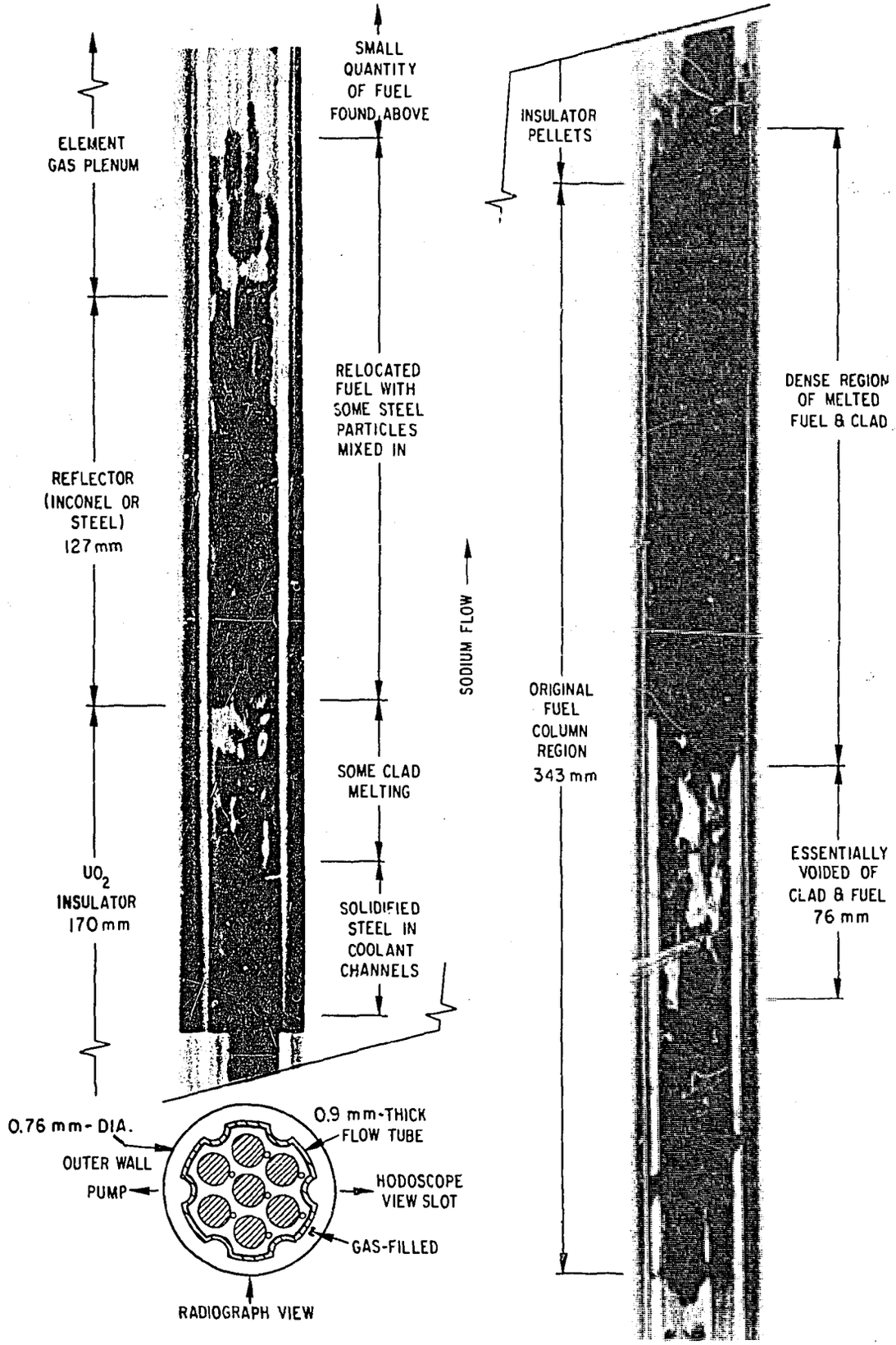

Fig. 2 Post-Test neutron radiograph of TREAT Test E8, compared to dissection examination.

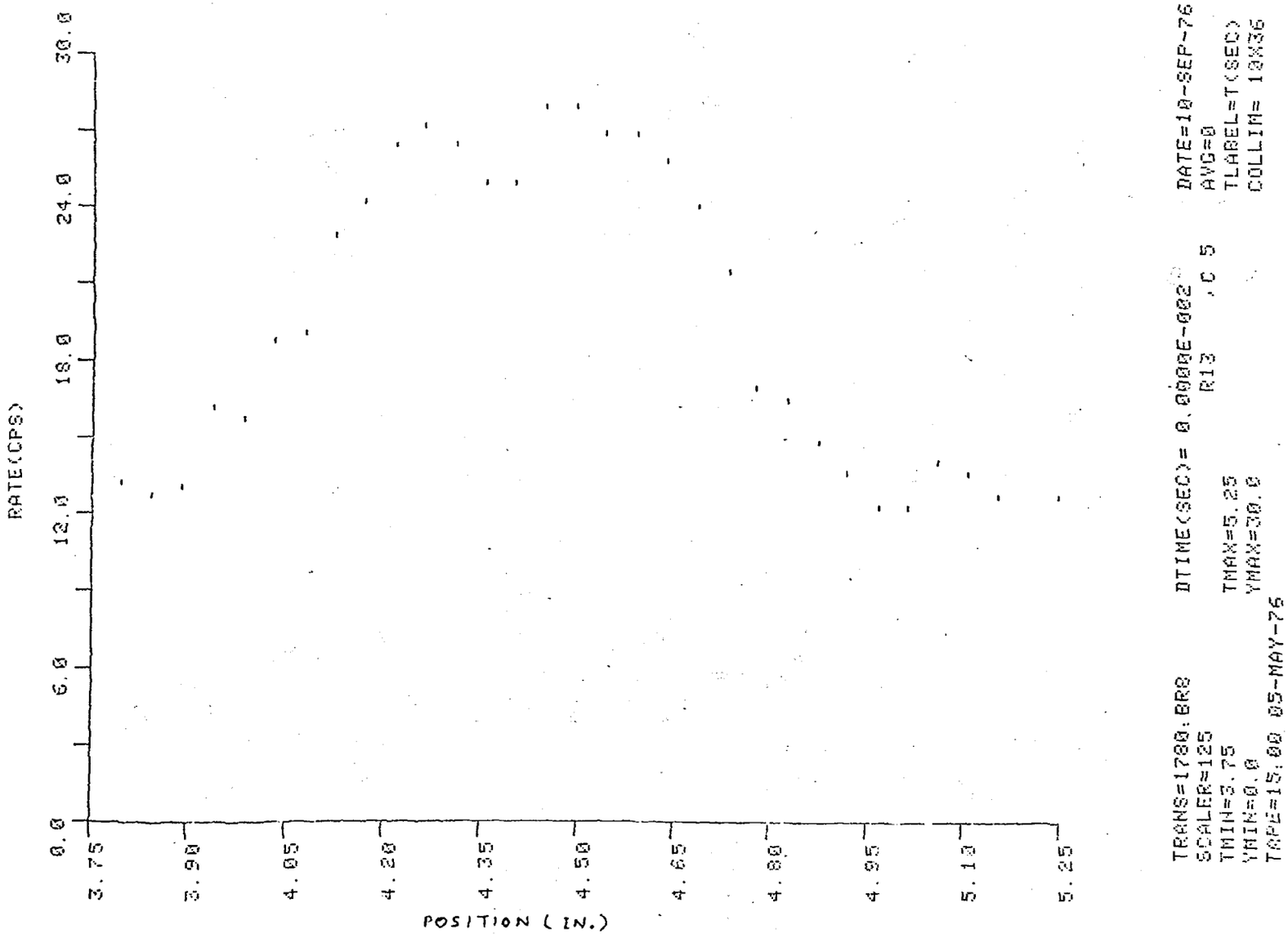

Fig. 3. Uncorrected pre-test horizontal scan over R8 7-pin test assembly by hodoscope detector in row 13, column 5.

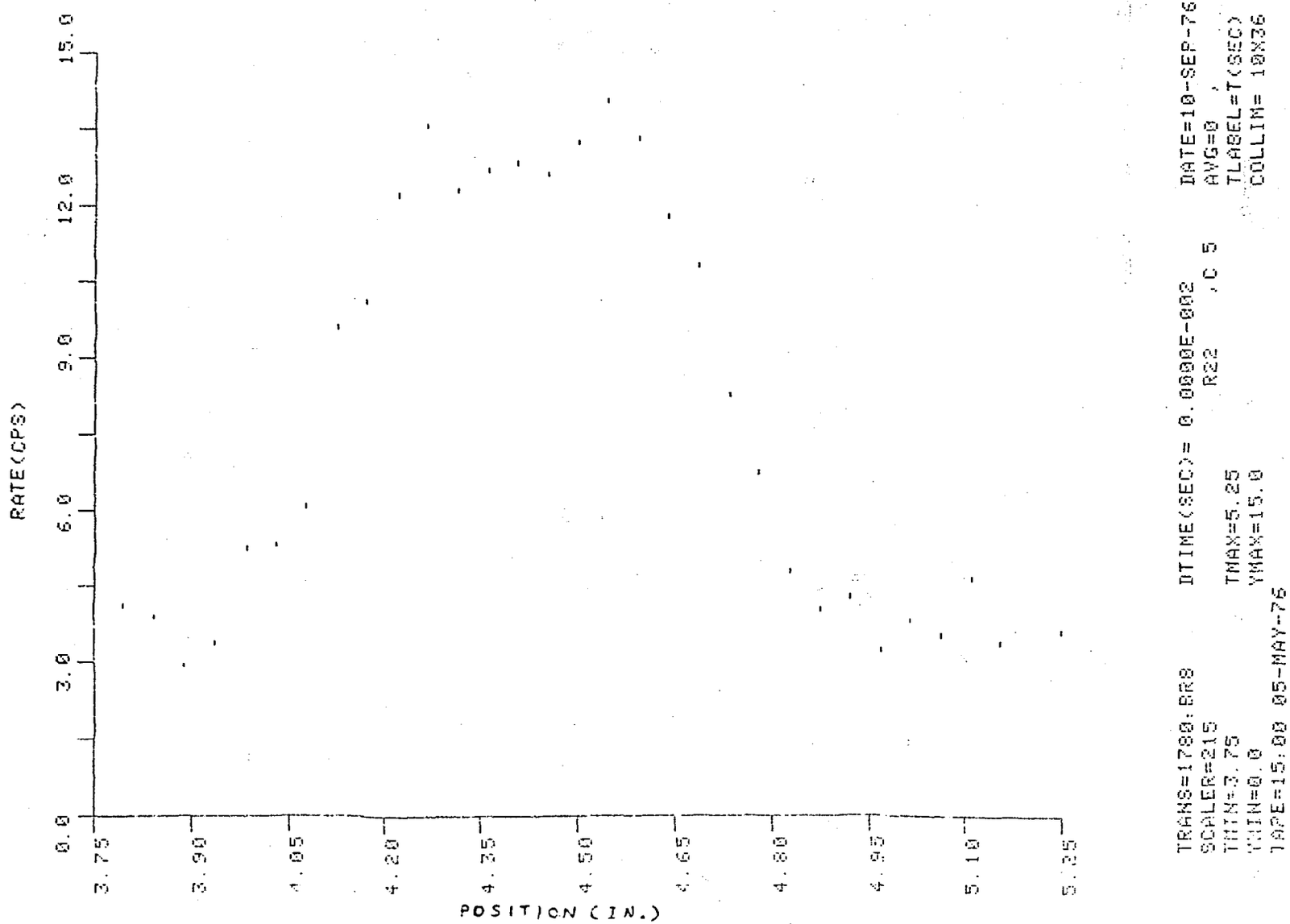

Fig. 4. Uncorrected pre-test horizontal scan over R8 7-pin test assembly by hodoscope detector in row 22, column 5.

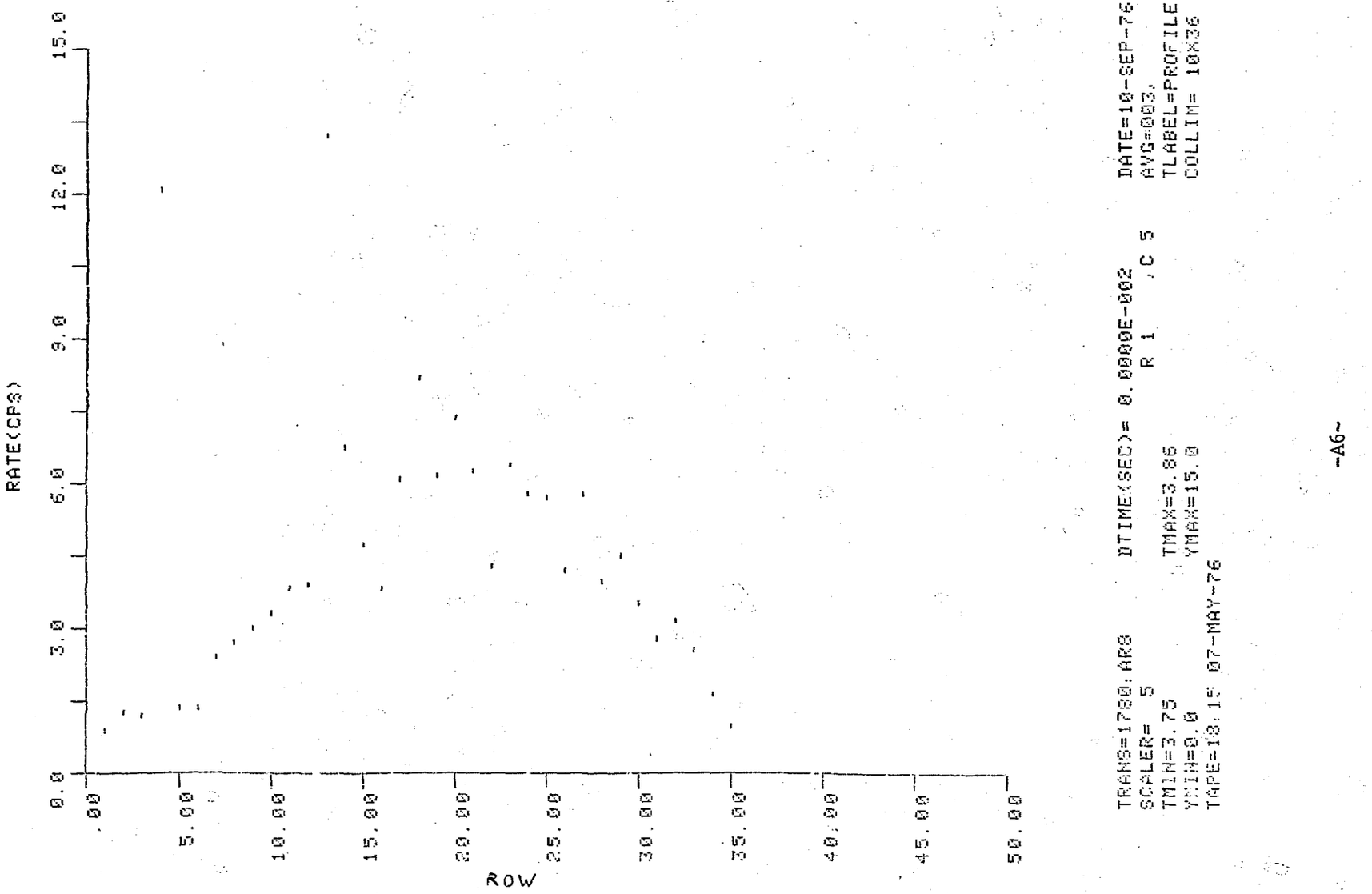

Fig. 5. Uncorrected post-test vertical profile over rows 1-35 of column 5 of hodoscope, averaged over background to left of R8 test assembly.

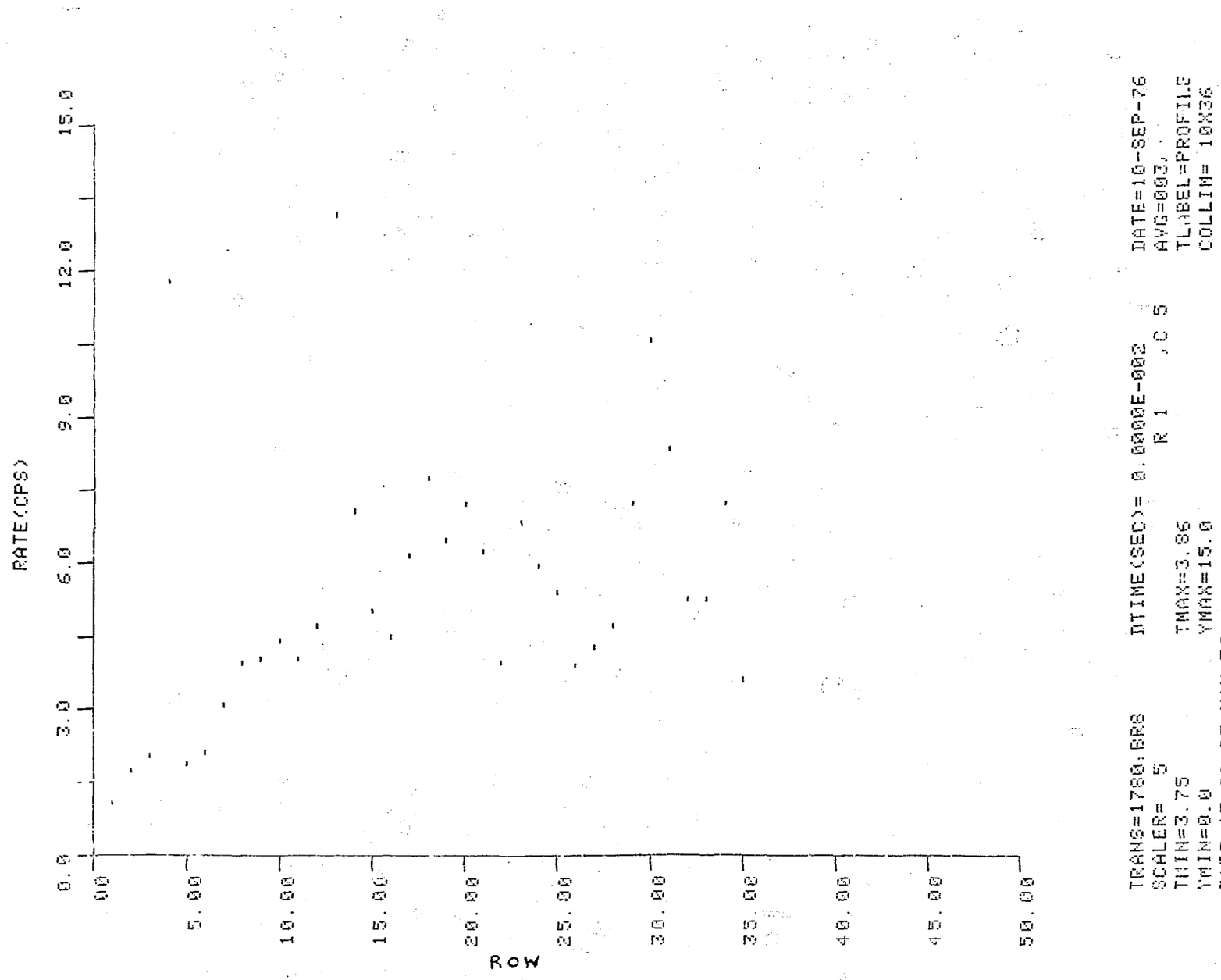

Fig. 6. Uncorrected pre-test vertical profile over rows 1-35 of column 5 of hodoscope, averaged over background to left of R8 test assembly.

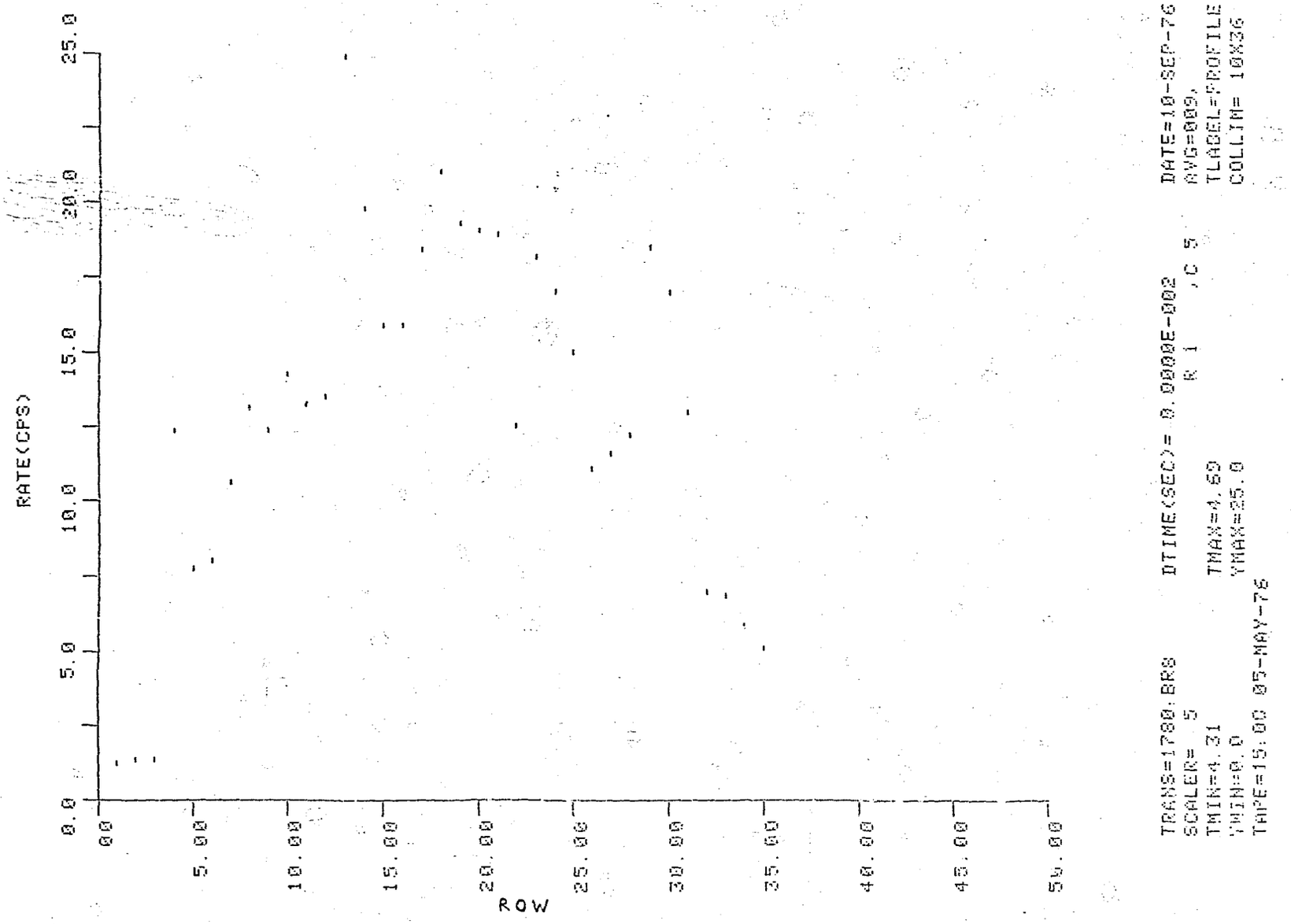

Fig. 7. Uncorrected pre-test vertical profile over rows 1-35 of column 5 of hodoscope, averaged over R8 test assembly.

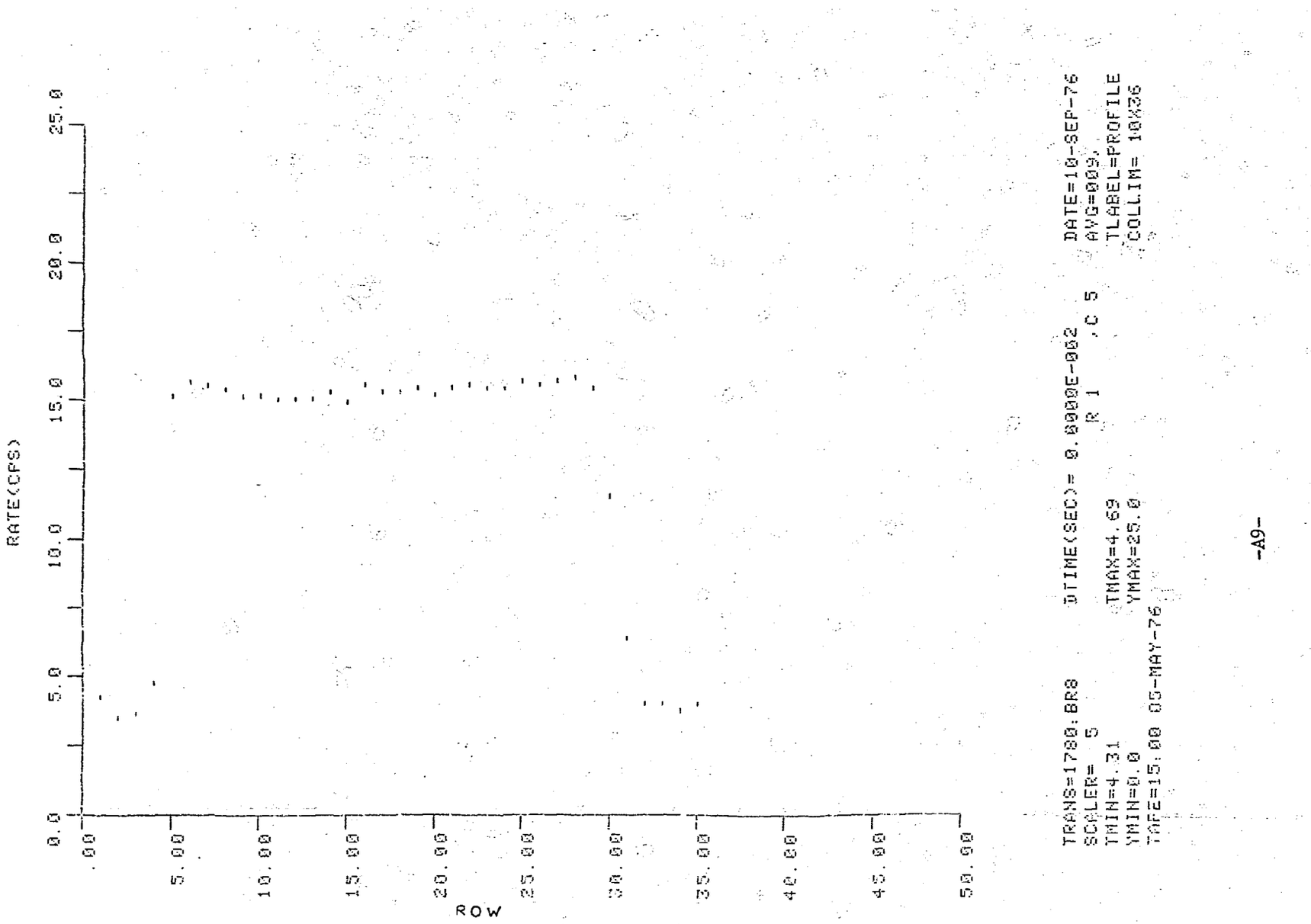

Fig. 8. Corrected pre-test vertical profile over rows 1-35 of column 5 of hodoscope, averaged over R8 test assembly.

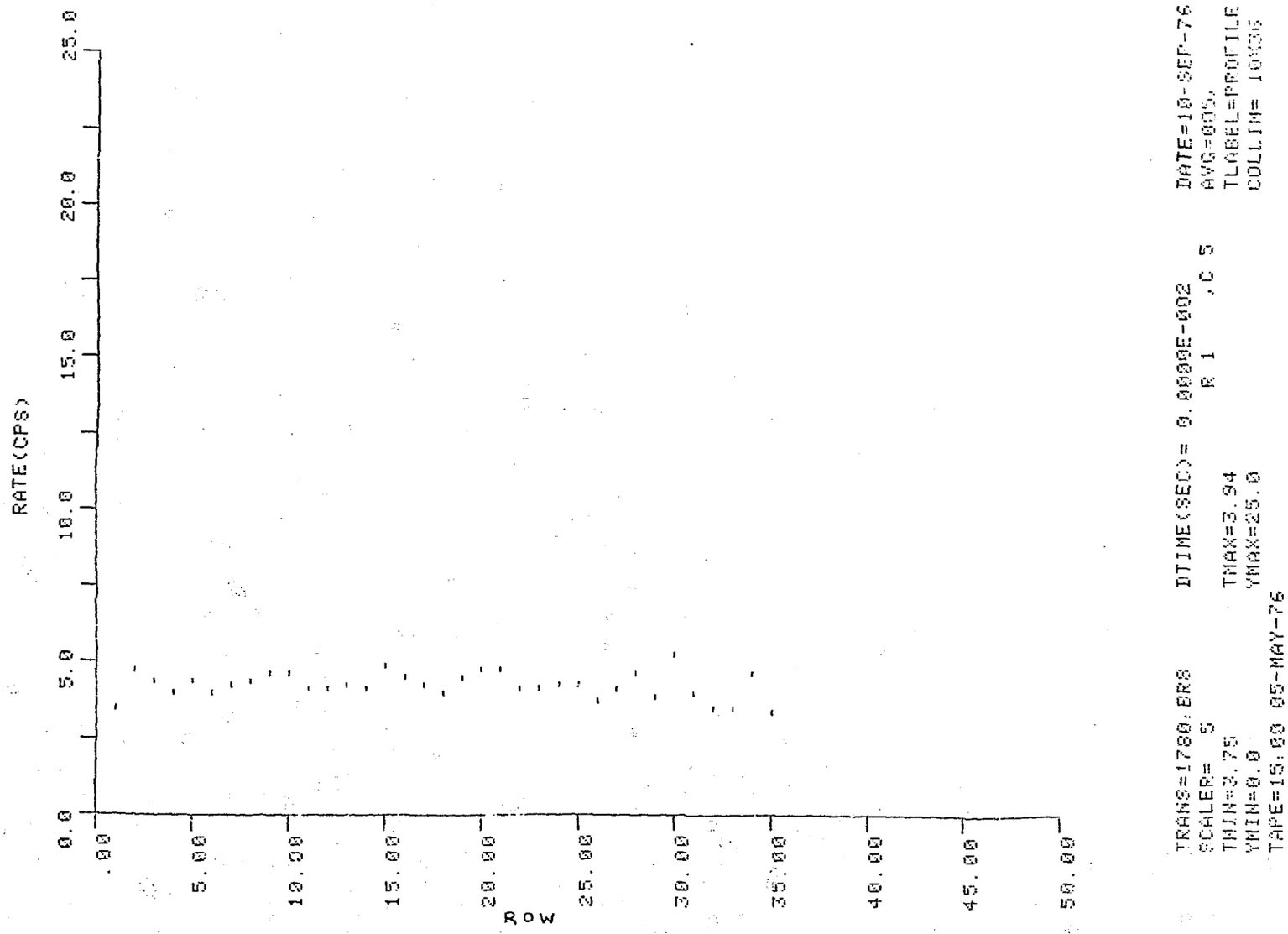

Fig. 9. Corrected pre-test vertical profile over rows 1-35 of column 5 of hodoscope, averaged over background to left of R8 test assembly.

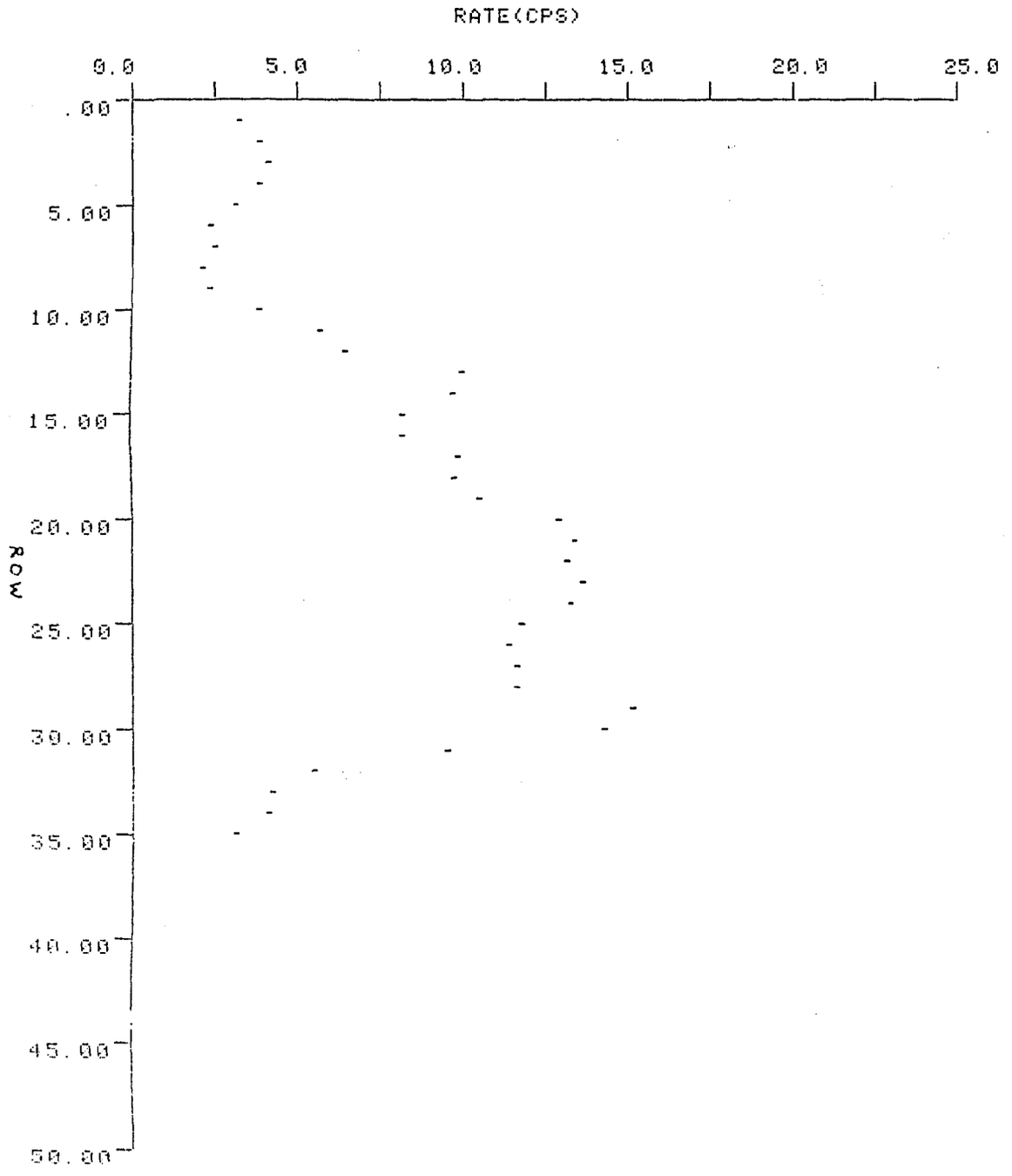

TRANS=1700:AR8 DTIME(SEC)= 0.0000E-002 DATE=10-SEP-76
SCALER= 5 R 1 ,C 5 AVG=023,
TMIN=3.86 TMAX=4.95 TLABEL=PROFILE
YMIN=0.0 YMAX=25.0 COLLIM= 10X36
TAPE=18:15 07-MAY-76

Fig. 10. Corrected post-test vertical profile over rows 1-35 of column 5 of hodoscope, averaged over R8 test assembly.

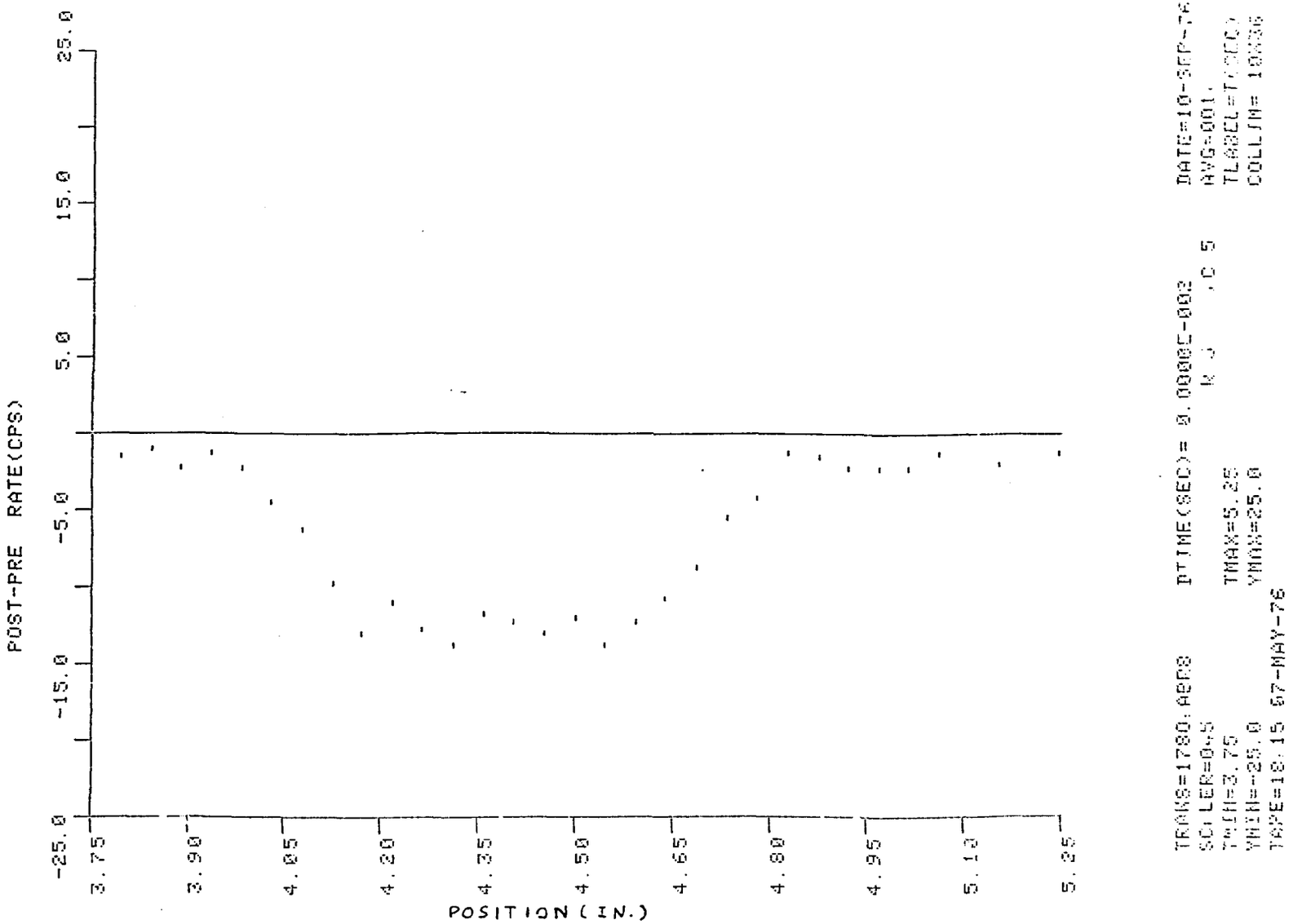

Fig. 11. Corrected post-test horizontal scan over R8 7-pin test assembly by hodoscope detector in row 5, column 5.

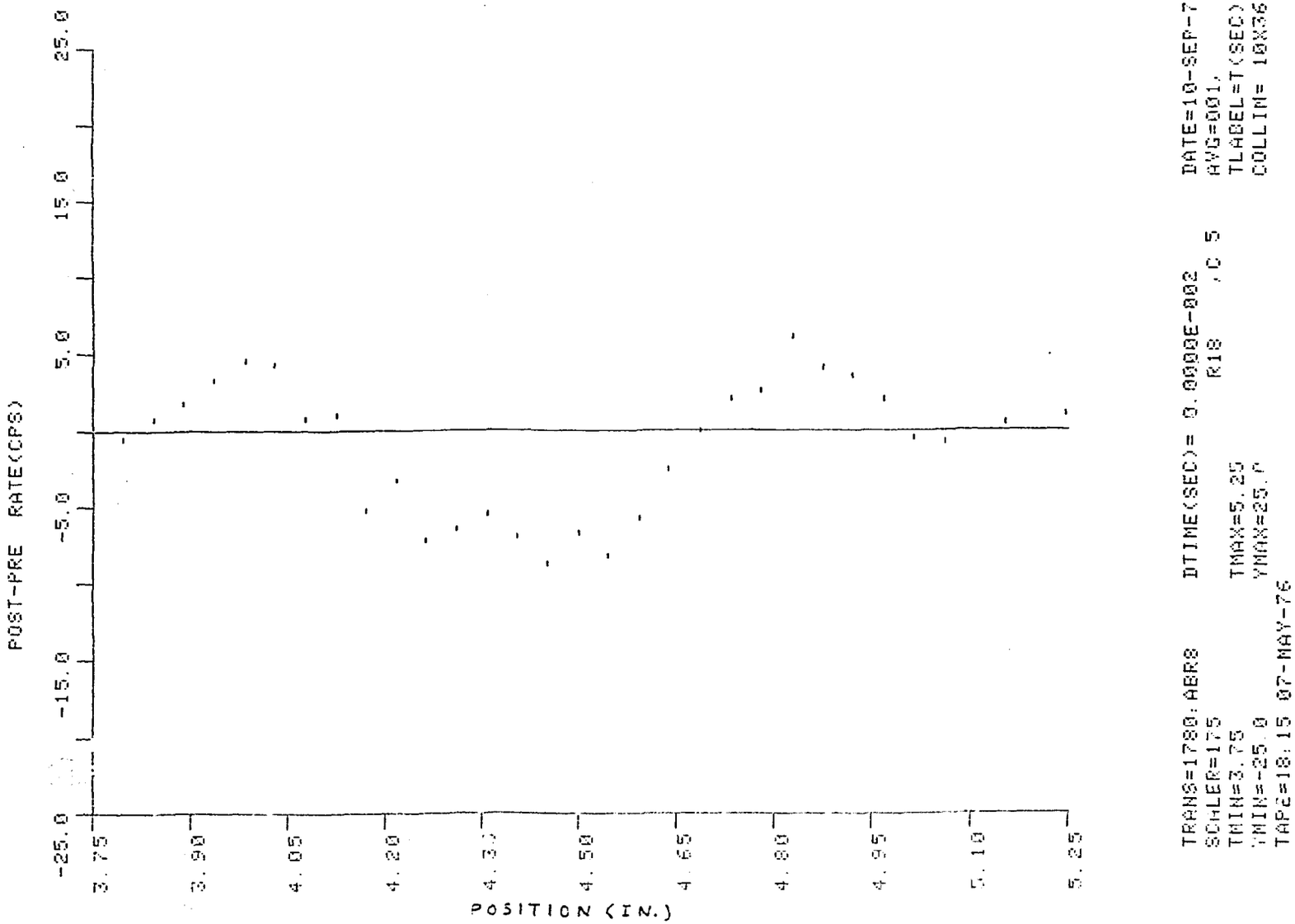

Fig. 12. Corrected post-test horizontal scan over R8 7-pin test assembly by hodoscope detector in row 18, column 5.

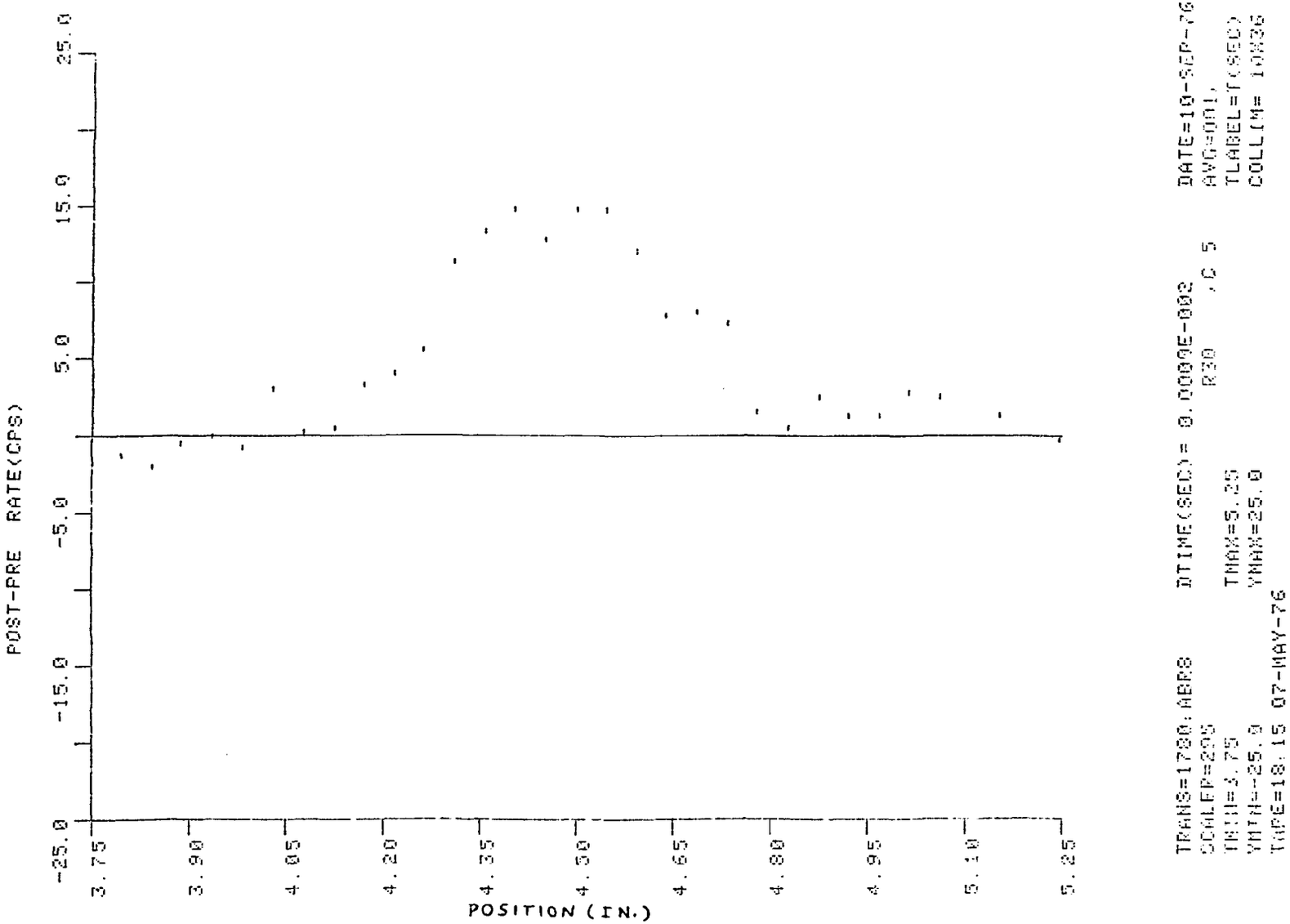

Fig. 13. Corrected post-test horizontal scan over R8 7-pin test assembly by hodoscope detector in row 30, column 5.

Fig. 14. Corrected pre-test intensity-modulated pseudo-radiograph of R8 7-pin test assembly, column of 36 detectors and 30 horizontal scan positions.

Fig. 15. Corrected post-test intensity-modulated pseudo-radiograph of R8 7-pin test assembly, column of 36 detectors and 30 horizontal scan positions.

ADDENDUM

HODOSCOPE IN-SITU RADIOGRAPHY

Following presentation of this paper at the meeting, a comment was made by H. Barrett that the deconvolution noise instability, using the method in Sec. III, is probably a good deal worse than assumed in Sec. V, perhaps requiring impractically long times to perform radiographic scans. The validity of this comment will be established by the computer experiments referred to in Sec. VII.3. If his comment is found to be valid, other deconvolution methods will be investigated. One potential technique, not mentioned in the text, is the maximum entropy algorithm (see Ref. 9 of text and * below).

Of course, the need for deconvolution could be eliminated by using an aperture having the required resolution, such as a hodoscope collimator with narrow slots or pinholes, or a simple pinhole. By combining such an aperture with a position-sensitive detection system, counting time could be reduced and scanning could be eliminated. However, the signal-to-background ratio would be substantially reduced, depending on the aperture and detector designs. The best system for in-situ radiography depends to a large extent on the required spatial and density resolutions, which are not yet established.

---

*B. Roy Frieden and William Swindell, "Restored Pictures of Ganymede, Moon of Jupiter", Science 191, p. 1237 (26 March 1976).